Environ Sci Pollut Res (2016) 23:18552–18563
DOI 10.1007/s11356-016-7031-4

RESEARCH ARTICLE

Application of TiO_2-organobentonite modified by cetyltrimethylammonium chloride photocatalyst and polyaluminum chloride coagulant for pretreatment of aging landfill leachate

Yi-Jie Zhang[1,2] · Zhao-Hui Yang[1,2] · Pei-Pei Song[1,2] · Hai-Yin Xu[1,2] · Rui Xu[1,2] · Jing Huang[1,2] · Juan Li[1,2] · Yan Zhou[1,2]

Received: 7 April 2016 / Accepted: 2 June 2016 / Published online: 13 June 2016

Abstract This study investigated the treatment performance for aging leachate containing refractory organic pollutants by TiO_2-organobentonite photocatalyst combined with polyaluminum chloride (PAC) coagulant. TiO_2 was immobilized on organobentonite granules as a supporter modified by cetyltrimethylammonium chloride (CTAC). The prepared catalysts were characterized by ESEM, FTIR, and XRD analysis, which showed that TiO_2-organobentonite catalyst had uniform coating of TiO_2 on support. Chemical oxygen demand (COD) and NH_3-N removal rates by combination of TiO_2-CTAC2.0 photocatalysis and PAC coagulation were evaluated, optimized, and compared to that by either treatment alone, with respect to TiO_2-CTAC2.0 dose, photocatalytic contact time, pH, and PAC dose. Furthermore, higher removal rates (COD 80 %; NH_3-N 46 %) were achieved by response surface methodology (RSM) when TiO_2-CTAC2.0 photocatalysis was followed by PAC coagulation at optimized conditions. The optimized experimental conditions were TiO_2-CTAC2.0 dosage of 5.09 g/L, at pH 5.53, photocatalytic contact time for 180 min, and PAC dosage of 1062 mg/L.

Responsible editor: Suresh Pillai

✉ Zhao-Hui Yang
yzh@hnu.edu.cn

[1] College of Environmental Science and Engineering, Hunan University, Changsha 410082, People's Republic of China

[2] Key Laboratory of Environmental Biology and Pollution Control (Hunan University), Ministry of Education, Changsha 410082, People's Republic of China

Keywords Aging leachate · TiO_2-CTAC2.0 · Photocatalysis · PAC · Coagulation · COD · NH_3-N

Introduction

Municipal solid waste (MSW) has been identified as one of the most serious environmental problems worldwide due to the excessive generation with rapid economic development (Giusti 2009). MSW is predominantly disposed in local sanitary landfills, which generate a highly contaminated wastewater called landfill leachate. The formation of leachate is mainly the percolation of rainfall in combination with the decomposition by a series of combined physico-chemical and biological processes. Landfill leachate is a high-strength wastewater exhibiting acute and chronic toxicity. Furthermore, the chemical compositions of leachate vary a lot depending on hydrogeology and climate of the site, age of landfill, composition of the MSW, and maturity of the landfill site (Peng et al. 2008). The main features of aging landfill leachate are a high strength of organic compounds, as described by chemical oxygen demand (COD), a high strength of ammonia nitrogen (NH_3-N) and a low biodegradability (BOD_5/COD ratio) (Deng and Englehardt 2006). Untreated leachate can pollute surface water and groundwater and contribute to potentially serious hazards on surrounding soil, water, and public health (Moreira et al. 2015).

Several technologies for landfill leachate remediation have been reported in recent decades (Renou et al. 2008). Biological processes are not effective for aging leachate with a low BOD_5/COD ratio (Uygur and Kargi 2004). Therefore, physico-chemical processes are frequently applied to the treatment of landfill leachate (Kurniawan et al. 2006b), such as coagulation/flocculation, adsorption, air stripping, chemical

oxidation processes, and membrane separation processes (Chianese et al. 1999). Additionally, advanced oxidation processes have been researched widely during recent years (Moreira et al. 2015; de Morais and Zamora 2005), such as ozone and ozone-based processes (Gao et al. 2015), TiO_2/UV photocatalysis (Cho et al. 2002), and Fenton (electro-Fenton, phono-Fenton) (Umar et al. 2010). Advanced oxidation processes have many advantages, including plant simplicity, adaptability in a wide pollutant concentration, and the ability of decomposing recalcitrant compounds in leachate (Peng et al. 2008). However, individual treatment is not effective enough to remove the bulk of refractory pollutants (Gotvajn et al. 2009); an integrated method to treat landfill leachate (Kurniawan and Lo 2009; Liu et al. 2015) is more and more applied, as the two treatments may synergize the advantages in treating leachate performance while overcoming their respective limitations (Kurniawan and Lo 2009).

Photocatalytic degradation has been proposed in wastewater treatment by several researchers (Wiszniowski et al. 2004). TiO_2 has been widely used in the photocatalytic reaction due to its excellent properties and ability of strong oxidation with respect to toxic organic substances in polluted aqueous systems (Poblete et al. 2011). Even if nanoparticle TiO_2 have many advantages, including chemical stability, nontoxicity and relatively inexpensive (Wang et al. 1998), their benefits are counteracted by drawbacks such as the aggregation, the loss and poor dispersivity (Shavisi et al. 2014). Many techniques have been applied for solving these problems, with immobilizing TiO_2 catalysts onto a suitable solid support. Up to now, various types of supports have been used, for example, adsorbent, natural mineral, glass, and organic material (Nagarajan and Rajendran 2009). In this regard, the use of mineral structure such as bentonite has attracted more and more attention because of their low-cost, easy availability, high cation exchange capacity, and high adsorption property (Zhu et al. 1998).

Bentonite is mainly composed of montmorillonite, and it has net negative charges on the surfaces due to isomorphic substitutions on the montmorillonite structure (Shen 2002). The exchange cations can compensate the negative charges and easily hydrate to form a thin water film (Baskaralingam et al. 2006; Cai et al. 2014), leading to a weak adsorption of nonionic organic matters. It is organobentonite that organic cations are intercalated into the lattice structure of bentonite, and its surfaces are transformed from hydrophilic to hydrophobic and formed sorptive phase (Baskaralingam et al. 2006). Meanwhile, organobentonite has a large pore volume and surface area, so it is advantageous to the formation of TiO_2-organobentonite. The photocatalytic activity of TiO_2-organobentonite is much higher than that of pure TiO_2 (Sun et al. 2002) because TiO_2-organobentonite granules have good adsorption with a porosity structure and good dispersivity that allow them to uniformly disperse in water. Nevertheless, the suspended TiO_2-organobentonite particles are still in the effluent, and the integrated treatment with other technologies such as coagulation/flocculation may improve its treatability.

Coagulation/flocculation is a relatively simple technique that has been employed successfully in the pretreatment of landfill leachate (Ghafari et al. 2009). Several studies (Tatsi et al. 2003) have been reported on the removal of organic matters and other pollutants from landfill leachate by coagulation/flocculation. The most common coagulants are various, such as aluminum sulfate, polyaluminum chloride, ferrous sulfate, and ferric chloride (Tatsi et al. 2003; Oloibiri et al. 2015). Among them, polyaluminum chloride (PAC) has a strong appeal due to a series of advantages, such as high coagulation precipitation speed, a wide pH range, and high efficiency for water purification.

In the previous studies, the leachate treatment by either photocatalysis or coagulation/flocculation was researched but the performance was not superior to its combination. Carlos Amor et al. (2015) verified that analogous combination of coagulation/flocculation and solar photo-Fenton processes had higher COD removal efficiency of 75 % compared to single solar photo-Fenton with 54 %. Until now, coagulation/flocculation was generally used as pretreatment process at the first stage, and rare attempt had been made to investigate the application of TiO_2-pillared organobentonite modified by CTAC for pretreatment of aging leachate. In this regard, an integrated method of TiO_2-organobentonite photocatalysis followed by PAC coagulation may be technically applicable, since it could simultaneously deal with original suspended matter and used TiO_2-organobentonite particles in leachate then reduce the burden and is cost saving for the subsequent processing in this way.

Therefore, the main aim of this study was the examination of the feasibility for pretreatment of aging landfill leachate by combined TiO_2-organobentonite photocatalysis with PAC coagulation. Firstly, the optimal preparation conditions of TiO_2-organobentonite were investigated. Secondly, this paper studied the feasibility of PAC coagulation followed TiO_2-organobentonite photocatalysis. The third goal was to find the optimal operation by response surface methodology.

Materials and methods

Materials

Cetyltrimethylammonium chloride (supplied by Kermel Chemical Reagent Development Center, Tianjin), as an organic modifier with long alkyl chain and cation exchange, is better for the modification of natural bentonite (from Shisihewei Chemical Co., Ltd., Shanghai). Butyl titanate (from Sinopharm Chemical Reagent Co., Ltd) as precursor was used in the preparation of TiO_2. All chemicals used in this work

were of analytical grade, including HNO_3, HCl, H_2SO_4, and NaOH.

In this study, aging leachate samples were collected from Heimifeng Landfill. This landfill, located in Changsha, China, covers about 174 ha surface, which has been in operation since 2003, and treats more than 5000 tons of solid waste daily. The characteristics of samples were shown in Table 1.

Sample preparation

Preparation of organobentonite

Organobentonite was prepared as follows: (1) 30 mL HCl and 45 mL H_2SO_4 were added into 925 mL distilled water; (2) 100 g natural bentonite was added into the mixture liquor; (3) mixture solution was magnetically stirred (ZNCL-S) at the speed of 500 r/min for 3 h at room temperature; (4) 0.75 g PAC, 0.05 g polyacrylamide (PAM), which were conductive to agglomerate and conglutinate organic modifier and bentonite (Cai et al. 2014), and a little CTAC ranged from 1.0 to 3.0 g/L were added into suspension obtained from the third step and the solution was magnetically stirred at the speed of 500 r/min for 5 h at 60 °C; (5) the solution was filtered by vacuum suction filter pump (SHZ-D(III)), and the precipitate was rinsed repeatedly with ultrapure water; (6) the precipitate was dried in the oven (101A-2) for 4 h at 90 °C and activated for 1 h at 110 °C, then milled into powder and sealed in a desiccator for further experiment tests.

Preparation of TiO_2-organobentonite

TiO_2-organobentonite was prepared as follows: (1) 20 mL butyl titanate was added into 80 mL absolute ethanol as the medium base; (2) a quantitative dilute nitric acid was added with pH 2 for inhibiting butyl titanate hydrolysis; (3) the mixture solution was magnetically stirred (ZNCL-S) at the speed of 300 r/min for 2 h at room temperature; (4) 20 g organobentonite was added to the mixture liquor, and the turbid liquid was magnetically stirred continuously at the speed of 300 r/min for 6 h; (5) 5 mL distilled water was added into 10 mL absolute ethanol and pH of the liquor was adjusted to 3; (6) the solution was slowly dropped to suspension obtained from the third step and was continuously stirred until gelation; (7) the gelation was allowed to stand and aged for 24 h, then dried in the oven (101A-2) for 12 h at 80 °C for the ethanol to evaporate slowly; (8) the dried gelation was milled into powder and calcinated at a certain temperature for 3 h, then sealed in a desiccator for further experimental tests. Optimal additive CTAC dosage and roasted temperature were determined by actual experiments operated under the same condition of 180 min reaction time, 4.0 g/L TiO_2-organobentonite dosage, and without pH adjustment of raw aging leachate.

Table 1 Properties of raw leachate

Constituent	Range	Average	Units
COD	4650–5050	4850	mg/L
BOD_5	680–810	750	mg/L
Ammonia	1900–2200	2050	mg/L
BOD/COD	0.13–0.17	0.15	
SS	79–94	87	mg/L
Color	400–500	450	PCU
pH	7.65–8.15	8.05	

Characterization of organobentonite and TiO_2-organobentonite

The surface morphologies and microscopic features of prepared TiO_2-organobentonite, organobentonite, and natural bentonite were determined using an environmental scanning electron microscope (ESEM)/energy dispersive spectrometer (EDS) (Quanta 200 FEG, USA). The Fourier transform infrared (FTIR) spectrum was recorded using 8400S FTIR spectrometer (IR prestige-21, Japan) to characterize the TiO_2, bentonite and prepared TiO_2-organobentonite photocatalysts and organobentonite. TiO_2-organobentonite phase structure was characterized by X-ray diffraction (XRD) (XRD-6100, Japan) measurement. Brunauer–Emmett–Teller (BET) surface area was measured by specific surface area and pore volume adsorption analyzer (OMNISORP100CX, USA).

Experimental procedure

The leachate was submitted to a TiO_2-organobentonite photocatalytic process in the first stage and subsequently treated by PAC coagulation. The efficiencies of integrated technique were evaluated, taking into account COD and NH_3-N evolution during the processes. Briefly, suitable amount of TiO_2-organobentonite photocatalyst was added in the reactor with ultraviolet (UV) irradiation, and then UV light was closed until the efficiencies reached equilibrium. Due to the addition of powdered TiO_2-organobentonite materials, suspended particles showed the poor effect of sedimentation and subsidence rate in natural conditions. So suitable amount of PAC was added into the reactor for coagulation and precipitation.

TiO_2-organobentonite photocatalytic reaction

Photocatalytic experiments were carried out in a self-designed cylindrical photocatalytic reactor (9 cm of internal diameter and 18 cm of height) with a total volume of 1000 mL, approximately. A 18-W low-pressure ultraviolet mercury vapor lamp (Xuelaite, ZW18D17Y) with two u-tubes (outer diameter of 1 cm, length of 13 cm) was set in the middle of the cylindrical reactor. The

intensity of UV light with peak emission at 365 nm was 57 μW/cm^2 within the range of 100 cm. There was a micro-aeration head so that the aeration was maintained at 0.8 L/min at the bottom of reactor. The aeration not only provided oxygen for photocatalytic oxidation but also maintained the photocatalyst in suspension state to enhance its contact with contaminants to improve degradation efficiency (Jia et al. 2011). Figure 1 schematically illustrated the reactor system. These experiments were performed with the change of the amount of TiO_2-organobentonite, initial pH, and reaction time to determine the best conditions of photocatalytic reaction.

PAC coagulation reaction

The turbid solution after photocatalytic reaction was magnetically stirred when added a certain amount of PAC into it, at the speed of 150 r/min for 15 min, followed by 50 r/min for 5 min. These experiments were performed with the change of the dosage of PAC.

RSM experiment design

The Design Expert Software (version 8.0.6) was used for the statistical design of experiments and data analysis. In this study, the central composite design (CCD), a response surface methodology (RSM), was applied to optimize the four most important operating variables: TiO_2-organobentonite dosage (x_1), pH (x_2), photocatalytic reaction time (x_3), and PAC dosage (x_4), respectively. The practical design operated was displayed in Table 2. In order to select the optimal conditions of variables, two dependent parameters were analyzed as responses: removal rates of COD and NH_3-N. All factors were controlled at five levels, and CCD was selected to frame 30 experiments. A second-order polynomial model for the response variable (y) can be expressed according to quadratic Eq. 1:

$$y = \beta_0 + \sum_{i=1}^{m} \beta_i x_i + \sum_{i<j}^{m} \beta_{ij} x_i x_j + \sum_{i=1}^{m} \beta_{ii} x_i^2 \quad (1)$$

where y is the response variable, i is the linear coefficient, j is the quadratic coefficient, β is the regression coefficient that reflects the interaction between x_i and x_j, m is the number of factors studied (Ghafari et al. 2009; Huang et al. 2012).

Table 2 Coded levels for 4 variables framed by central composite design (CCD)

Factor	Codes	Coded levels				
		−2	−1	0	1	2
TiO_2-bentonite (g/L)	x_1	1.5	3	4.5	6	7.5
pH	x_2	2	3.5	5	6.5	8
Time (min)	x_3	0	60	120	180	240
PAC (mg/L)	x_4	0	400	800	1200	1600

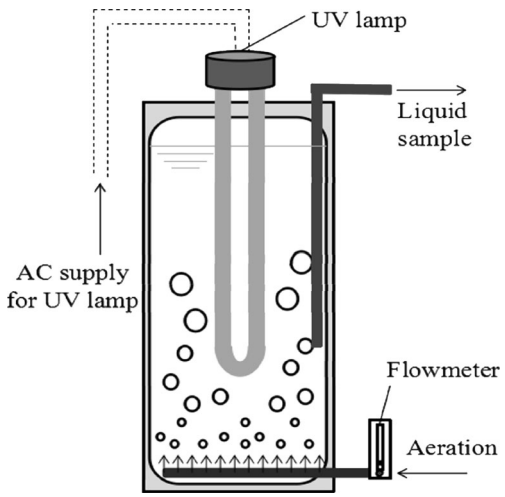

Fig. 1 Schematic diagram of the reactor apparatus used in this study

Results and discussion

Analysis of optimal condition for photocatalyst

The organobentonite modified by the additive of CTAC ranged from 1.0 to 3.0 g/L. The obtained TiO_2-organobentonite composite was calcined at different temperatures, 300, 400, 500, and 600 °C. Results were shown in Fig. 2. Obviously, COD and NH_3-N removal rates firstly ascended with increasing CTAC dosage; after reaching a peak, COD and NH_3-N removal rates slightly declined with further CTAC dosage under 300, 400, and 500 °C; the best efficiencies were at 500 °C. COD and NH_3-N removal rates had been descended and presented irregular change at 600 °C. The adsorption performance and photocatalytic effect of TiO_2-organobentonite were greatly reduced when the temperature reached at 600 °C. According to Fig. 2, the efficiencies became better with the optimal CTAC dosage of 2.0 g and 500 °C calcined, so organobentonite was defined as CTAC2.0, and the final photocatalyst was defined as TiO_2-CTAC2.0.

Testing of treated leachate with used TiO_2-CTAC2.0 under the same condition showed similar COD and NH_3-N removal performances after multiple tests. Reused times were more than 3. Therefore, the result indirectly revealed that the level of TiO_2 particle released from CTAC2.0 was limited and TiO_2-CTAC2.0 had the value of repeated use (Cai et al. 2014).

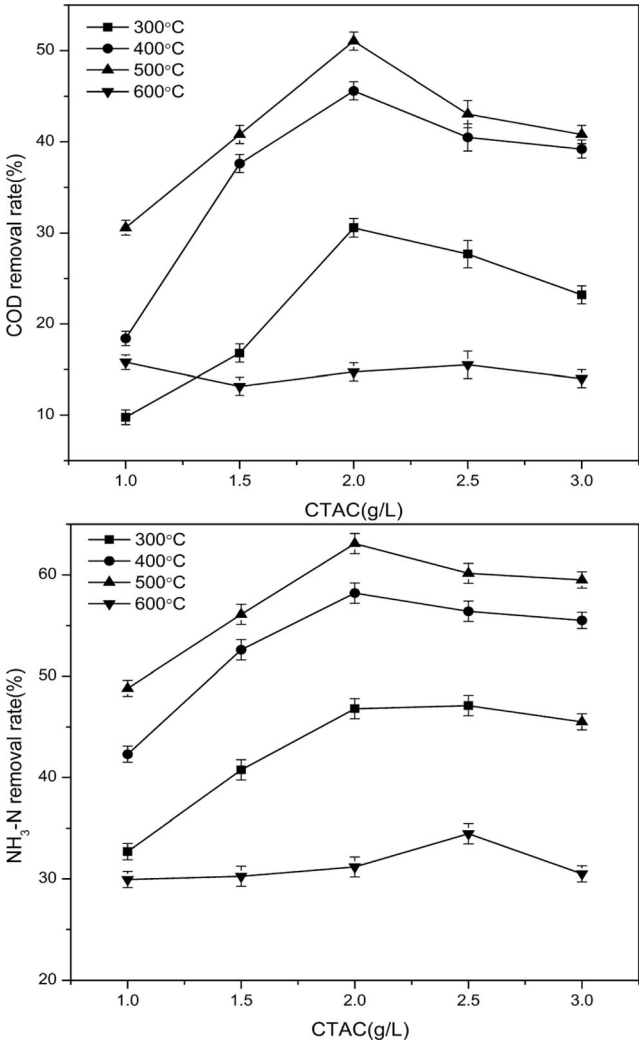

Fig. 2 The effect of CTAC dosage and calcined temperature for TiO_2-organobentonite on COD and NH_3-N removal rates

Characteristic analysis of TiO_2-CTAC2.0

Natural bentonite which is used as the supporter was shown in Fig. 3a. This image clarified that natural bentonite had a smooth surface structure. Figure 3b showed the surface of bentonite after organically modified by CTAC. This image showed the CTAC2.0 surface was rugged. EDS analysis declared that carbon elementary contents of CTAC2.0 in Fig. 3e relatively increased than natural bentonite in Fig. 3d. It clarified that CTAC cation had been successfully modified on the surfaces of bentonite. After high temperature roasting, organic functional groups should have completely oxidative decomposition. EDS analysis confirmed that carbon elementary contents of TiO_2-CTAC2.0 in Fig. 3f shrunk down to almost nothing. So in Fig. 3c, the dispersed TiO_2 nanoparticles were mostly coated on the external surfaces of organobentonite. Similar results of the immobilized TiO_2 had been reported on different supports (Eliyas et al. 2013).

Figure 4 showed the FTIR spectra of natural bentonite, CTAC2.0, TiO_2, and TiO_2-CTAC2.0 photocatalyst, respectively. Obvious differences displayed between natural bentonite and CTAC2.0 were two adsorption bands at 2920 and 2850 cm^{-1}. Adsorption bands of CTAC around at 2920 and 2850 cm^{-1} correspond to CH_2 asymmetric stretch modes and CH_3 symmetric stretch modes, respectively (Hu and Luo 2010). Thus, CTA^+ was successfully loaded on natural bentonite surface; its surfaces were transformed from hydrophilic to hydrophobic and formed sorptive phase, then absorption property of bentonite was improved and it was advantageous to the formation of TiO_2-organobentonite. The IR spectrum of the TiO_2-CTAC2.0 was not the same as the TiO_2 due to IR band differences at 3800–3000 and 800–770 cm^{-1}. The absorption bands at 3800–3000 cm^{-1} revealed a large amount of adsorbed H_2O and surface OH groups on the CTAC2.0 surface, and the intensity of the peaks at 800–770 cm^{-1} was related to Si-O-Si bands. This indicated that TiO_2 particles had been effectively loaded on the surface of the organobentonite granules.

X-ray diffraction pattern that showed diffraction peaks of CTAC2.0 was weakened in comparison with natural bentonite, and TiO_2-CTAC2.0 kept the characteristic peaks in Fig. 5. This also showed that the structure of bentonite had not collapsed at 500 °C, and the dispersed TiO_2 particles were mostly loaded on the surface of CTAC2.0. Meanwhile, X-ray diffraction pattern of TiO_2-CTAC2.0 showed strong diffraction peaks at 2θ values 25.38, 37.84, 48.07, and 55.10 corresponding to the phases of (101), (004), (200), and (211) (Ghasemi et al. 2013). These peaks were the characteristic peaks of titanium dioxide present on the surface of the substrate. From the diffraction peaks, the crystalline phase was identified as the anatase phase (Nagarajan and Rajendran 2009).

The BET surface area, pore volume, and average pore size of natural bentonite, CTAC2.0, and TiO_2-CTAC2.0 were displayed in Table 3. As shown in Table 3, the BET surface area of TiO_2-CTAC2.0 (135 m^2/g) was larger than that of natural bentonite (119 m^2/g), which explained that TiO_2 was successfully grafted on CTAC2.0 and increased the surface area of TiO_2-CTAC2.0. Besides, the obvious difference was porosity, but it had no significant difference for porosity of CTAC2.0 when TiO_2 was loaded. The porosity of CTAC2.0 and TiO_2-CTAC2.0 was higher than that of natural bentonite, and the result inferred that its adsorption was better.

The various mechanisms of TiO_2-CTAC2.0 proposed for adsorption and decomposition of refractory organic pollutants (ROPs) were summarized in Fig. 6.

Combination of TiO_2-CTAC2.0 photocatalysis and PAC coagulant

The combination of TiO_2-CTAC2.0 photocatalysis and PAC coagulation was clearly superior to others according to Fig. 7.

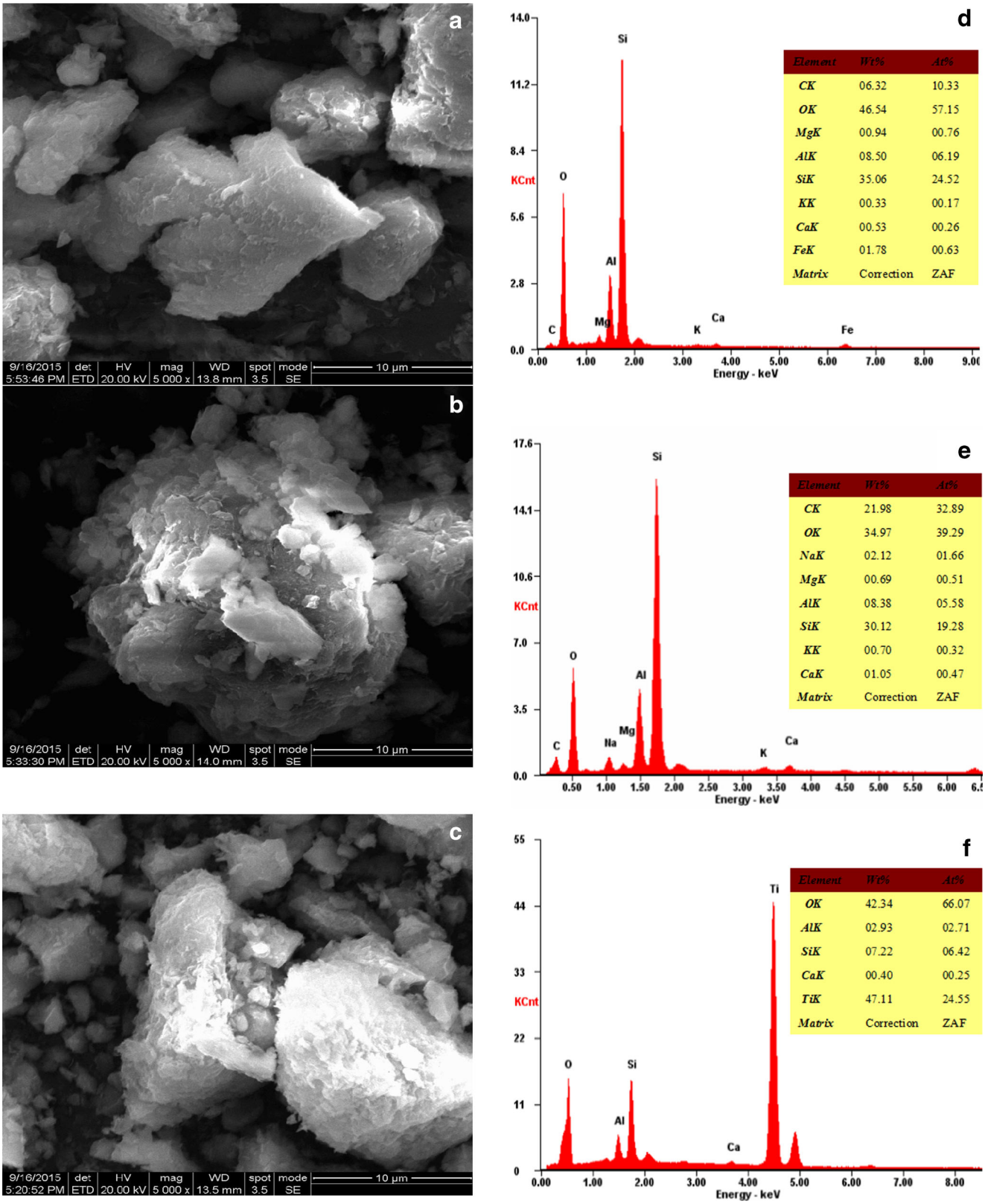

Fig. 3 Environment scanning election microscope grasps at ×5000 and energy dispersive spectrometer analysis graphs: **a** and **d** natural bentonite, **b** and **e** CTAC2.0, **c** and **f** TiO_2-CTAC2.0

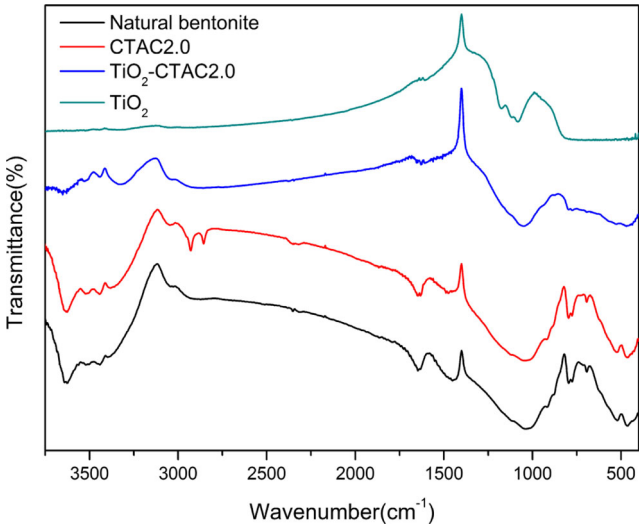

Fig. 4 Fourier transform infrared spectra of natural bentonite, CTAC2.0, TiO_2-CTAC2.0, and pure TiO_2

In combination of 4.5 g/L TiO_2-CTAC2.0 and 800 mg/L PAC, the optimal removal rates of COD and NH_3-N were up to 89 and 42 %, respectively. In comparison with pure TiO_2 powder, the performance of TiO_2-CTAC2.0 was enhanced mainly due to surface transition to hydrophobic and strong adsorption and dispersion of CTAC2.0. In addition, due to well dispersion and poor sedimentation performance of bentonite, the solution was still in the suspended state after the photocatalytic reaction for some time, so TiO_2-CTAC2.0 photocatalysis alone showed low COD and NH_3-N removal rates.

Additionally, in order to compare the effect of the photocatalysis and coagulation in different sequences on pretreatment of landfill leachate, TiO_2-CTAC2.0 photocatalysis and PAC coagulation were divided two successive steps at pH 5. When PAC coagulation was

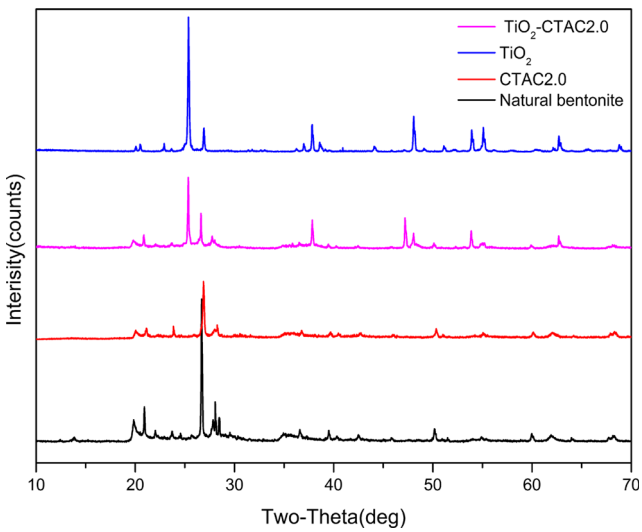

Fig. 5 X-ray diffraction of natural bentonite, CTAC2.0, TiO_2-CTAC2.0, and TiO_2

Table 3 Selected physical properties of natural bentonite, CTAC2.0, and TiO_2-CTAC2.0

Samples	BET surface area (m^2/g)	Porosity (%)	Pore size (nm)
Natural bentonite	119	59	1350
CTAC2.0	122	71	1560
TiO_2-CTAC2.0	135	70	1550

followed by photocatalysis treated with TiO_2-CTAC2.0, the solution was still a suspension after the reaction, and the suspended matter would bring significant influence on removal rates of COD and NH_3-N, so that the removal rates of COD and NH_3-N were 57 and 28 %, respectively. Otherwise, when 4.5 g/L TiO_2-CTAC2.0 photocatalyst and 800 mg/L PAC were added simultaneously, the removal rates of COD and NH_3-N were 45 and 22 %, respectively. Owing to the TiO_2-CTAC2.0 photocatalyst that grew into larger particles with the coagulation of PAC, the photocatalytic effectiveness was greatly reduced. In comparison with removal rates of 85 % COD and 42 % NH_3-N, TiO_2-CTAC2.0 photocatalysis prior to PAC coagulation was the best choice for pretreatment of landfill leachate.

For the comparison of adsorption and photocatalysis performance with catalyst and support, a series of experiments were set in the dark or UV irradiation at the same time. The experimental results were shown in Fig. 8. The absorption property of CTCA2.0 was improved, but TiO_2 supported on organobentonite may not greatly improve the adsorption property of organobentonite. The photocatalytic activity of TiO_2-

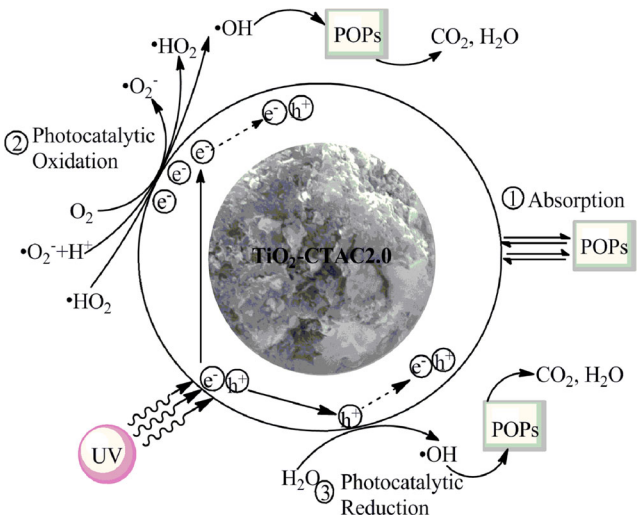

Fig. 6 The schematic illustration of refractory organic pollutants' (ROPs) adsorption and decomposition mechanisms on TiO_2-CTAC2.0

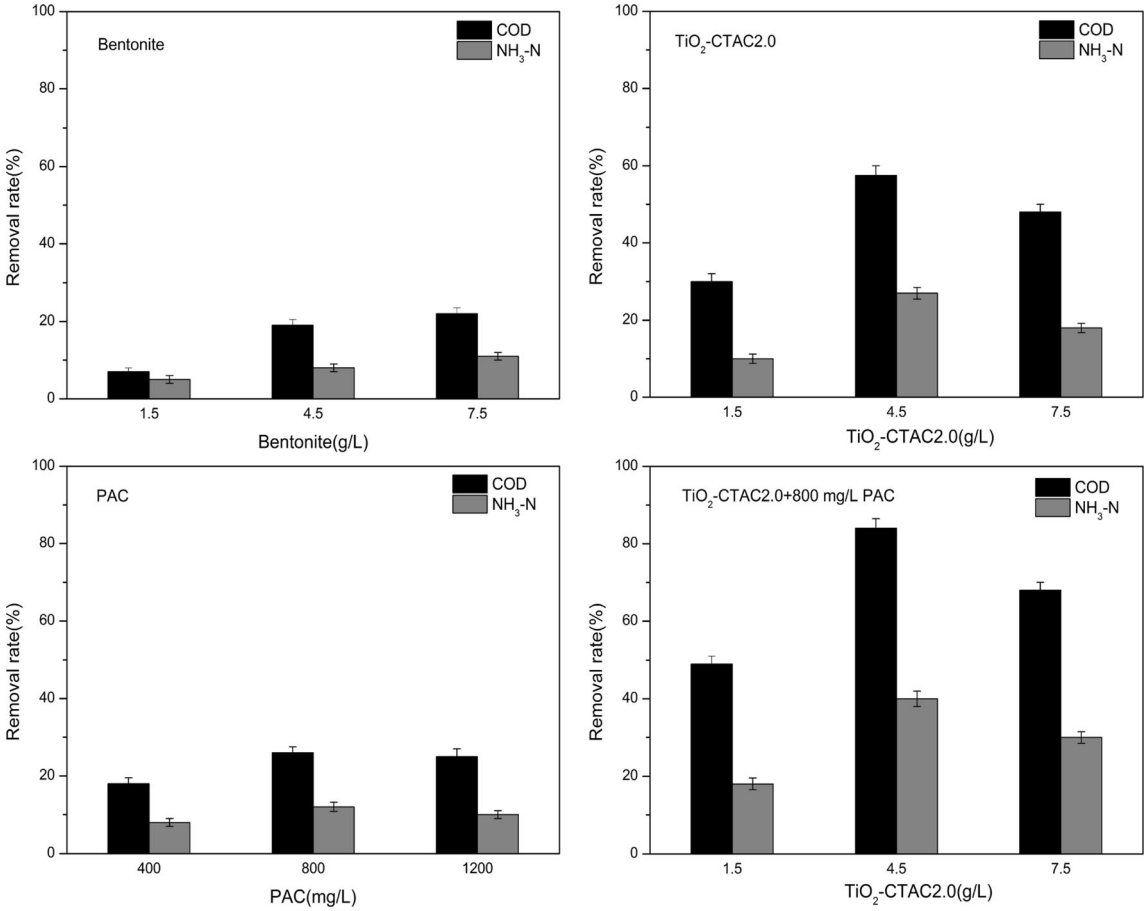

Fig. 7 The different removal rates of COD and NH_3-N among four groups at pH 5

CTAC2.0 was much higher than that of pure TiO_2 and TiO_2-bentonite because TiO_2-organobentonite granules had good dispersivity that allowed them to uniformly disperse in water and more fully utilized ultraviolet irradiation.

Considering that aeration may influence the disappearance of NH_3-N, a series of experiments were conducted. In fact, NH_3-N removal rates almost kept invariably with aeration ranging from 0.4 to 1.2 L/min, and the removal rates improved no more than 2 % ($p \leq 0.05$, paired t test) at the condition of 4.5 g/L TiO_2-CTAC2.0, pH of 5, 180 min photocatalytic reaction time, and 800 mg/L PAC,. Thus, aeration was not a major influence factor for NH_3-N removal; so experiments were conducted at 0.8 L/min to keep the photocatalyst in suspension state.

RSM experimental data analysis

The relationship between four variables (TiO_2-CTAC2.0 dosage, pH, photocatalytic reaction time, and PAC dosage) and two responses (COD and NH_3-N removal rates) was analyzed using RSM. Response variables of COD and NH_3-N removal rates were acquired from 30 groups of experiments. The results were summarized in Table 4.

Data analysis of COD removal as the response variable

The quadratic equation model for the relationship between COD removal rates and four operating variables (x_1–x_4) could be expressed as Eq. 2:

$$y_1 = +70.13 + 8.21x_1 - 4.52x_2 + 11.92x_3 + 4.46x_4 + 0.69x_1x_2 - 1.56x_1x_3 + 2.19x_1x_4 + 1.5x_2x_3 - 0.062x_2x_4 - 0.062x_3x_4 - 9.04x_1^2 - 6.02x_2^2 - 3.96x_3^2 - 3.66x_4^2 \quad (2)$$

The statistical testing of the model was then analyzed by ANOVA to assess the "goodness of fit" (Ghafari et al. 2009). Table 5 illustrated the analytical results. Data given in Table 5 demonstrated that the model was significant because the value of Prob > F < 0.0001 was less than 0.05, and total determination coefficient reached

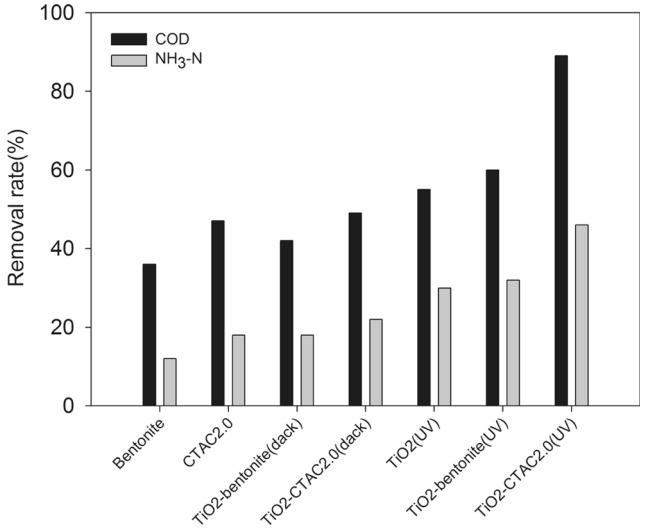

Fig. 8 The comparison of catalyst and support in adsorption and photocatalysis performance with dosage of materials = 5.00 g/L, reaction time = 3 h, pH = 5, PAC = 800 mg/L

0.8494. The lack of fit (LOF) described the variation of the data around the obtained model. The *p* value for lack of fit (>0.05) showed that the *F*-statistic was insignificant, implying the model correlation between the variables and COD removal rates.

The response surface plots for COD and NH_3-N removal rates were shown in Fig. 9. Figure 9a clearly showed COD removal rates with the variation of TiO_2-CTAC2.0 dosage and pH. The interaction between TiO_2-CTAC2.0 dosage and pH mutually influenced COD removal rates. Figure 9c clearly showed COD removal rates with the variation of TiO_2-CTAC2.0 dosage and PAC dosage. The response plots showed clear peak, implying that the optimum condition for COD maximum removal was attributed to TiO_2-CTAC2.0 dosage and pH in the design space. Obviously, when added a certain amount of TiO_2-CTAC2.0, COD removal firstly ascended with decreasing pH, and after reaching a peak, COD removal slightly declined. Because organic pollutants were in stable state in alkaline environment, these were hard to be degraded. While in acid conditions, TiO_2-CTAC2.0 was strongly favored to adsorb pollution and also generated electron-hole pair and hydroxylation, then accelerated the formation of •OH and the occurrence of photooxidation (Kurniawan et al. 2006a). However, the aluminum salt was almost in the form of Al^{3+} ion in water at pH < 4 because of aluminum hydroxide dissolved in water. The Al^{3+} ions had no

Table 4 CCD design and response values

Run	Coded levels				Real values				Response	
	x_1	x_2	x_3	x_4	x_1	x_2	x_3	x_4	COD removal rate (%)	NH_3-N removal rate (%)
1	−1	1	1	1	3	6.5	180	1200	40	30
2	−1	1	1	−1	3	6.5	180	400	39	30
3	−1	−1	1	1	3	3.5	180	1200	45	13
4	0	2	1	0	4.5	8	180	800	52	65
5	0	0	0	2	4.5	5	120	1600	77	34
6	1	1	−1	1	6	6.5	60	1200	48	20
7	0	0	1	0	4.5	5	180	800	89	42
8	−1	−1	1	−1	3	3.5	180	400	53	12
9	1	−1	1	1	6	3.5	180	1200	72	23
10	0	−2	0	0	4.5	2	120	800	63	10
11	−1	−1	−1	−1	3	3.5	60	400	25	9
12	1	1	1	−1	6	6.5	180	400	55	42
13	0	0	0	0	4.5	5	120	800	71	31
14	−1	−1	−1	1	3	3.5	60	1200	34	7
15	0	0	0	−2	4.5	5	120	0	45	32
16	1	1	−1	−1	6	6.5	60	400	39	10
17	0	1	1	0	4.5	6.5	180	800	74	54
18	−1	1	−1	−1	3	6.5	60	400	20	12
19	−1	1	−1	1	3	6.5	60	1200	22	13
20	2	0	0	0	7.5	5	120	800	49	13
21	1	−1	−1	−1	6	3.5	60	400	52	14
22	1	1	1	1	6	6.5	180	1200	64	48
23	1	−1	1	−1	6	3.5	180	400	53	20
24	0	0	0	0	4.5	5	120	800	73	32
25	0	0	−2	0	4.5	5	0	800	26	11
26	0	0	2	0	4.5	5	240	800	91	45
27	0	0	−1	0	4.5	5	60	800	45	16
28	−2	0	0	0	1.5	5	120	800	30	12
29	1	−1	−1	1	6	3.5	60	1200	54	13
30	0	1	0	0	4.5	6.5	120	800	51	47

Table 5 ANOVA for COD removal analysis of variance and significant items of the quadratic model

Source	Sum of squares	*df*	Mean square	*F* value	Prob > *F*
Model	8723.5	14	623.11	6.04	0.0007
x_1	1617.04	1	1617.04	15.68	0.0013
x_2	498.98	1	498.98	4.84	0.0439
x_3	3836.59	1	3836.59	37.21	< 0.0001
x_4	477.04	1	477.04	4.63	0.0483
x_1^2	2003.97	1	2003.97	19.43	0.0005
x_2^2	822.17	1	822.17	7.97	0.0128
Residual	1546.80	15	103.12		
Lack of fit	1544.80	14	110.34	55.17	0.1052
Pure error	2.00	1	2.00		

$SD = 10.15$, $R^2 = 0.8494$, $Adj\ R^2 = 0.7088$, $Adeq\ R^2 = 8.548$

adsorption so that particulate matter could not bond together, and the COD removal would be affected with pH at a low level. Furthermore, COD removal firstly ascended with advancing TiO_2-CTAC2.0 dosage; after reaching a peak, COD removal slightly declined. When TiO_2-CTAC2.0 dose was high, photocatalytic oxidation played lesser role in degrading COD than its adsorption performance. The reasons were that the suspended TiO_2-CTAC2.0 particles located closer to the radiation source had taken place and the TiO_2-CTAC2.0 particles intercepted the penetration of UV light toward the solution, and the light might be scattered by suspended solid in the landfill leachate.

The maximum COD removal rate reached 89 % with TiO_2-CTAC2.0 dose of 4.5 g/L, pH of 5, reaction time for 180 min, and PAC dosage of 800 mg/L in 30 sets of experiments.

Data analysis of NH_3-N removal as the response variable

The quadratic equation model between NH_3-N removal rates and four operating variables (x_1–x_4) could be represented in the form of Eq. 3:

$$y_2 = +33.09 + 2.75x_1 + 7.54x_2 + 8.61x_3 + 0.92x_4 + 0.37x_1x_2 + 2.00x_1x_3 + 1.13x_1x_4 + 5.41x_2x_3 + 1.00x_2x_4 + 0.1x_3x_4 - 6.21x_1^2 - 1.76x_2^2 - 2.15x_3^2 - 1.09x_4^2 \quad (3)$$

Results of analyzed by ANOVA were shown in Table 6. Data given in Table 6 implied that the second-order equation model fitted well because the value of Prob > F < 0.0001 was less than 0.05 and the total determination coefficient reached 0.9255. The LOF described the variation of the data around the obtained model. The p value for lack of fit (>0.05) reached 0.0890 presented in Table 6. The result showed that the F-statistic was insignificant, implying the model correlation between the variables and NH_3-N removal rates.

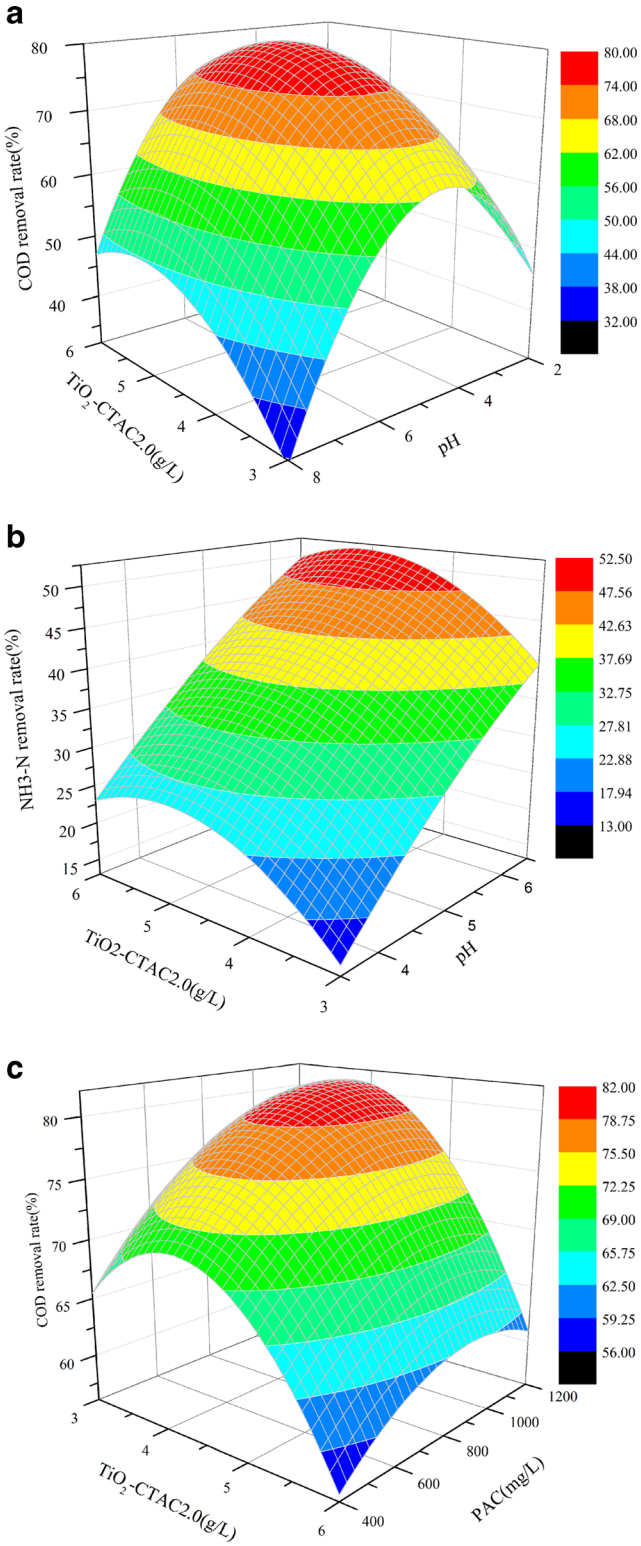

Fig. 9 The response surface plots of COD and NH_3-N removal rates: **a** and **b** removal rates with the variation of TiO_2-CTAC2.0 dosage and pH, reaction time = 180 min, and PAC dosage =800 mg/L; (c) COD removal rates with the variation of TiO_2-CTAC2.0 dosage and PAC, reaction time = 180 min, and pH = 5

Table 6 ANOVA for NH_3-N removal analysis of variance and significant items of the quadratic model

Source	Sum of squares	*df*	Mean square	*F* value	Prob > *F*
Model	6718.24	14	479.87	13.32	<0.0001
x_1	181.50	1	181.50	4.66	0.0403
x_2	1384.47	1	1384.47	38.43	<0.0001
x_3	2001.37	1	2001.37	55.55	<0.0001
x_2x_3	531.45	1	531.45	14.75	0.0016
x_1^2	946.28	1	946.28	26.26	0.0001
Residual	540.43	15	36.03		
Lack of fit	539.93	14	38.57	77.13	0.0890
Pure error	0.50	1	0.50		

SD = 6.00, R^2 = 0.9255, *Adj* R^2 = 8561, *Adeq* R^2 = 13.108

Figure 9b clearly showed that the interaction between TiO_2-CTAC2.0 dosage and pH mutually influenced NH_3-N removal rates. NH_3-N removal rates were predominantly affected by the pH of landfill leachate. The decomposition rates of NH_3-N in landfill leachate at high pH were significantly higher than at low pH. The results agreed with similar reports (Cho et al. 2002; Shavisi et al. 2014). At low pH, the large amount of hydrogen ions with smaller radius could compete the adsorption sites on the TiO_2-CTAC2.0 with ammonia ions with larger radius. With the advance of pH, the addition of OH^- would enhance the adsorption of ammonia by TiO_2-CTAC2.0 and availed to generate •OH to promote photocatalytic reaction. In addition, at high pH, ammonia in the form of NH_3 could be stripped with aeration. However, due to the effect of pH on the coagulation of PAC, the NH_3-N removal would be affected with pH at a high level. Aluminum hydroxide dissolved in the form of $Al(OH)_4^-$ ion in water at pH > 8, so the coagulation effect was not favorable.

The optimal NH_3-N removal rate arrived at 65 % with TiO_2-CTAC2.0 dose of 4.5 g/L, pH of 8, reaction time for 180 min, and PAC dosage of 800 mg/L in 30 sets of experiments.

Analysis of simultaneous removal of COD and NH_3-N

According to the experiments, with UV irradiation from 365 nm 18 W ultraviolet lamp, COD could be degraded to a significant extent at low pH and the ammonium-nitrogen compounds could be removed quickly at high pH. According to RSM, 80 % COD and 46 % NH_3-N were removed at the optimal operation condition of TiO_2-CTAC2.0 dose of 5.09 g/L, pH of 5.53, reaction time for 180 min, and PAC dosage of 1062 mg/L, corresponding to the values of COD and NH_3-N removal arrived at 84 and 44 % in verification experiment. Moreover, the experiments were mostly conducted in acid condition, which was a conductive environment for organic compounds removal rate; however, it hindered the removal of ammonia nitrogen. So by adjusting the pH of landfill leachate, we could emphasize to remove COD or NH_3-N in actual application. However, in consideration of PAC coagulation, pH of landfill leachate could not be overly acidic or alkali; the effluent turbidity, COD, and NH_3-N removal were subject to be affected.

Table 7 A comparison of raw aging leachate and effluent

Index	COD (mg/L)	NH_3-N (mg/L)	BOD_5 (mg/L)	BOD/COD
Raw aging leachate	4850	2050	750	*0.15*
Effluent	970	1109	388	*0.4*

Comprehensive analysis

After pretreatment of stabilized landfill leachate by combined TiO_2-CTAC2.0 photocatalyst with PAC coagulant under the optimal operation condition, COD, NH_3-N, BOD_5, and BOD/COD ratio of the treated effluent were 970 mg/L, 1107 mg/L, 388 mg/L, and 0.15, while COD, NH3-N, BOD5, and BOD/COD ratio of the raw aging leachate were 4850 mg/L, 2050 mg/L, 750 mg/L, and 0.4. This implied that the biodegradability of leachate was improved, with an increase in BOD_5/COD ratio from 0.15 to 0.40. These indexes of raw aging leachate and effluent were compared in Table 7. Considering that the COD and NH_3-N in the effluent were not complied with the standards (MEP 1990, 2009, 2010), then biochemical treatment as further treatment was allowed to treat the effluent.

Conclusions

Through the characterization of TiO_2-CTAC2.0 by ESME/EDS, FTIRS, and XRD, it confirmed that TiO_2 was successfully loaded on the surfaces of CTAC2.0 and improved the photocatalytic performance. Furthermore, the adsorption was improved by the success of the organic modification of bentonite. The application of TiO_2-CTAC2.0 photocatalysis technology and PAC coagulation technology was superior to either running alone. The removal rates of TiO_2-CTAC2.0 photocatalysis followed by PAC coagulation were superior to other sequence experiments.

These experiments showed that the maximum removal rate of COD was reached 89 % under TiO_2-CTAC2.0 dose of 4.5 g/L, pH of 5, reaction time for 180 min, and PAC dosage of 800 mg/L, and the maximum NH_3-N removal rate was arrived at 65 % with TiO_2-CTAC2.0 dose of 4.5 g/L, pH of 8, reaction time for 180 min, and PAC dosage of 800 mg/L. According to RSM, COD and NH_3-N removal rates were 80 and 46 % at the optimal operation condition of TiO_2-CTAC2.0 dose of 5.09 g/L, pH of 5.53, reaction time for 180 min, and PAC dosage of 1062 mg/L.

Acknowledgments This study was sponsored by the National Natural Science Foundation of China (Grant Nos. 51378189, 51578223, and 51521006).

References

Amor C, De Torres-Socías E, Peres JA, Maldonado MI, Oller I, Malato S, Lucas MS (2015) Mature landfill leachate treatment by coagulation/flocculation combined with Fenton and solar photo-Fenton processes. J Hazard Mater 286:261–268

Baskaralingam P, Pulikesi M, Elango D, Ramamurthi V, Sivanesan S (2006) Adsorption of acid dye onto organobentonite. J Hazard Mater 128:138–144

Cai FF, Yang ZH, Huang J, Zeng GM, Wang LK, Yang J (2014) Application of cetyltrimethylammonium bromide bentonite–titanium dioxide photocatalysis technology for pretreatment of aging leachate. J Hazard Mater 275:63–71

Chianese A, Ranauro R, Verdone N (1999) Treatment of landfill leachate by reverse osmosis. Water Res 33:647–652

Cho SP, Hong SC, Hong S-I (2002) Photocatalytic degradation of the landfill leachate containing refractory matters and nitrogen compounds. Appl Catal B Environ 39:125–133

De Morais JL, Zamora PP (2005) Use of advanced oxidation processes to improve the biodegradability of mature landfill leachates. J Hazard Mater 123(1):181–186

Deng Y, Englehardt JD (2006) Treatment of landfill leachate by the Fenton process. Water Res 40:3683–3694. doi:10.1016/j.watres.2006.08.009

Eliyas AE, Ljutzkanov L, Stambolova ID, Blaskov VN, Vassilev SV, Razkazova-Velkova EN, Mehandjiev DR (2013) Visible light photocatalytic activity of TiO2 deposited on activated carbon. Cent Eur J Chem 11:464–470

Gao JL et al. (2015) Integration of autotrophic nitrogen removal, ozonation and activated carbon filtration for treatment of landfill leachate. Chem Eng J 275:281–287. doi:10.1016/j.cej.2015.04.012

Ghafari S, Aziz HA, Isa MH, Zinatizadeh AA (2009) Application of response surface methodology (RSM) to optimize coagulation-flocculation treatment of leachate using poly-aluminum chloride (PAC) and alum. J Hazard Mater 163:650–656. doi:10.1016/j.jhazmat.2008.07.090

Ghasemi S, Esfandiar A, Setayesh SR, Habibi-Yangjeh A, Gholami M (2013) Synthesis and characterization of TiO 2–graphene nanocomposites modified with noble metals as a photocatalyst for degradation of pollutants. Appl Catal A Gen 462:82–90

Giusti L (2009) A review of waste management practices and their impact on human health. Waste Manag 29:2227–2239. doi:10.1016/j.wasman.2009.03.028

Gotvajn AZ, Tisler T, Zagorc-Koncan J (2009) Comparison of different treatment strategies for industrial landfill leachate. J Hazard Mater 162:1446–1456. doi:10.1016/j.jhazmat.2008.06.037

Huang J, Yang ZH, Zeng GM, Ruan M, Xu HY, Gao WC, et al. (2012) Influence of composite flocculant of PAC and MBFGA1 on residual aluminum species distribution. Chem Eng J 191:269–277

Hu B, Luo H (2010) Adsorption of hexavalent chromium onto montmorillonite modified with hydroxyaluminum and cetyltrimethylammonium bromide. Appl Surf Sci 257:769–775. doi:10.1016/j.apsusc.2010.07.062

Jia C, Wang Y, Zhang C, Qin Q (2011) UV-TiO_2 photocatalytic degradation of landfill leachate. Water Air Soil Pollut 217:375–385

Kurniawan TA, Lo W-h, Chan G (2006a) Radicals-catalyzed oxidation reactions for degradation of recalcitrant compounds from landfill leachate. Chem Eng J 125:35–57

Kurniawan TA, Lo WH (2009) Removal of refractory compounds from stabilized landfill leachate using an integrated H_2O_2 oxidation and granular activated carbon (GAC) adsorption treatment. Water Res 43:4079–4091. doi:10.1016/j.watres.2009.06.060

Kurniawan TA, Lo WH, Chan GY (2006b) Physico-chemical treatments for removal of recalcitrant contaminants from landfill leachate. J Hazard Mater 129:80–100. doi:10.1016/j.jhazmat.2005.08.010

Liu Z, Wu W, Shi P, Guo J, Cheng J (2015) Characterization of dissolved organic matter in landfill leachate during the combined treatment process of air stripping, Fenton, SBR and coagulation. Waste Manag 41:111–118

Moreira FC, Soler J, Fonseca A, Saraiva I, Boaventura RA, Brillas E, Vilar VJ (2015) Incorporation of electrochemical advanced oxidation processes in a multistage treatment system for sanitary landfill leachate. Water Res 81:375–387

Nagarajan S, Rajendran N (2009) Surface characterisation and electrochemical behaviour of porous titanium dioxide coated 316L stainless steel for orthopaedic applications. Appl Surf Sci 255:3927–3932. doi:10.1016/j.apsusc.2008.10.058

Oloibiri V, Ufomba I, Chys M, Audenaert WT, Demeestere K, Van Hulle SW (2015) A comparative study on the efficiency of ozonation and coagulation–flocculation as pretreatment to activated carbon adsorption of biologically stabilized landfill leachate. Waste Manag 43:335–342

Peng Y, Zhang S, Zeng W, Zheng S, Mino T, Satoh H (2008) Organic removal by denitritation and methanogenesis and nitrogen removal by nitritation from landfill leachate. Water Res 42:883–892. doi:10.1016/j.watres.2007.08.041

Poblete R, Otal E, Vilches LF, Vale J, Fernández-Pereira C (2011) Photocatalytic degradation of humic acids and landfill leachate using a solid industrial by-product containing TiO_2 and Fe. Appl Catal B Environ 102:172–179. doi:10.1016/j.apcatb.2010.11.039

Renou S, Givaudan JG, Poulain S, Dirassouyan F, Moulin P (2008) Landfill leachate treatment: review and opportunity. J Hazard Mater 150(3):468–493

Shavisi Y, Sharifnia S, Hosseini SN, Khadivi MA (2014) Application of TiO_2/perlite photocatalysis for degradation of ammonia in wastewater. J Ind Eng Chem 20:278–283. doi:10.1016/j.jiec.2013.03.037

Shen Y-H (2002) Removal of phenol from water by adsorption–flocculation using organobentonite. Water Res 36:1107–1114

Sun Z, Chen Y, Ke Q, Yang Y, Yuan J (2002) Photocatalytic degradation of a cationic azo dye by TiO_2/bentonite nanocomposite. J Photochem Photobiol A Chem 149:169–174

Tatsi AA, Zouboulis AI, Matis KA, Samaras P (2003) Coagulation–flocculation pretreatment of sanitary landfill leachates. Chemosphere 53:737–744. doi:10.1016/s0045-6535(03)00513-7

Umar M, Aziz HA, Yusoff MS (2010) Trends in the use of Fenton, electro-Fenton and photo-Fenton for the treatment of landfill leachate. Waste Manag 30:2113–2121. doi:10.1016/j.wasman.2010.07.003

Uygur A, Kargi F (2004) Biological nutrient removal from pre-treated landfill leachate in a sequencing batch reactor. J Environ Manag 71:9–14. doi:10.1016/j.jenvman.2004.01.002

Wang K-h, Hsieh Y-h, Chen L-j (1998) The heterogeneous photocatalytic degradation, intermediates and mineralization for the aqueous solution of cresols and nitrophenols. J Hazard Mater 59:251–260

MEP 2010 Water quality–Determination of ammonia nitrogen–Nessler's reagent spectrophotometry, HJ 535-2009

MEP 2009 Water quality–Determination of biochemical oxygen demand after 5 days (BOD5) for dilution and seeding method, HJ 505-2009

MEP 1990 Water quality–Determination of the chemical oxygen demand–Dichromate method GB, 11914-89

Wiszniowski J, Robert D, Surmacz-Gorska J, Miksch K, Malato S, Weber J-V (2004) Solar photocatalytic degradation of humic acids as a model of organic compounds of landfill leachate in pilot-plant experiments: influence of inorganic salts. Appl Catal B Environ 53:127–137. doi:10.1016/j.apcatb.2004.04.017

Zhu L, Ren X, Yu S (1998) Use of cetyltrimethylammonium bromide-bentonite to remove organic contaminants of varying polar character from water. Environ Sci Technol 32:3374–3378